Revista Mexicana de Astronomía y Astrofísica, **31**, 131-142 (1995)

THE EFFECT OF TEMPERATURE FLUCTUATIONS ON THE DETERMINATION OF THE CARBON ABUNDANCE OF PLANETARY NEBULAE

M. Peimbert, S. Torres-Peimbert, and V. Luridiana

Instituto de Astronomía
Universidad Nacional Autónoma de México

Received 1995 April 28; accepted 1995 August 7

RESUMEN

A partir de las intensidades de C III $\lambda\lambda$1906+1909 y las de C II λ4267 es posible determinar $T(C^{++})$; en las nebulosas planetarias esta temperatura es en general menor que $T(O^{++})$, la temperatura obtenida a partir del cociente $I(4363)/I(5007)$ de O III. Estudiamos las causas que puedan producir esta diferencia. Demostramos que en presencia de fluctuaciones espaciales de temperatura $T(C^{++}) < T(O^{++})$. Encontramos que los objetos en los que $T(O^{++}) - T(C^{++})$ es mayor son aquellos que muestran altas velocidades en sus envolventes, lo cual sugiere que la energía mecánica depositada por los vientos estelares es la causa de la diferencia. Basados en los argumentos anteriores y en la similitud de $T(C^{++})$, $T(\mathrm{Bac})$ y $T(\mathrm{He\ I})$ proponemos que la determinación de $N(C^{++})/N(H^{+})$ y de $N(O^{++})/N(H^{+})$ por medio de líneas de C^{++} y O^{++} excitadas colisionalmente se debe realizar a partir de $T(C^{++})$ en lugar de $T(O^{++})$. Por otro lado, los valores de $N(C^{++})/N(H^{+})$ y de $N(O^{++})/N(H^{+})$ determinados a partir de cocientes de líneas de recombinación son casi independientes de la temperatura adoptada y son más confiables que los obtenidos a partir de líneas colisionales.

ABSTRACT

By combining the C III $\lambda\lambda1906 + 1909$ with the C II λ4267 line intensities it is possible to determine $T(C^{++})$; this temperature is, in general, considerably smaller than $T(O^{++})$, the temperature derived from the O III λ4363 to λ5007 intensity ratio. We study possible causes for this difference. We show that in the presence of spatial temperature fluctuations $T(C^{++}) < T(O^{++})$. We find that the objects with the highest $T(O^{++}) - T(C^{++})$ values are those that show large velocities and complex velocity fields, therefore we suggest that the deposition of mechanical energy by the stellar winds of PNe is the main responsible for the temperature differences. Based on these arguments and the similar $T(C^{++})$, $T(\mathrm{Bac})$ and $T(\mathrm{He\ I})$ values, obtained for well observed objects, we propose that the $N(C^{++})/N(H^{+})$ and $N(O^{++})/N(H^{+})$ values derived from the ratio of collisionally excited lines to Hβ should be based on $T(C^{++})$ instead of $T(O^{++})$; alternatively the abundance ratios derived from recombination line intensity ratios are almost independent of the adopted temperature, and consequently are more reliable.

Key words: **PLANETARY NEBULAE — ISM–ABUNDANCES**

1. INTRODUCTION

The $N(C^{++})/N(H^{+})$ values derived from the C II λ4267 to Hβ intensity ratio are, in general, higher than those derived from the $\lambda\lambda1906 + 1909$ to Hβ intensity ratio; in some cases the difference reaches a factor of ten. General discussions of this problem have been given in the literature (e.g., Torres-Peimbert, Peimbert, & Daltabuit 1980; Kaler 1986; Rola & Stasinska 1994 and references therein). Several ideas have been advanced to explain the discrepancy: a) errors in the atomic data, b) errors in the observations, and c) the presence of spatial temperature fluctuations. To explain the presence of temperature fluctuations, considerably higher than those predicted by chemically homogeneous photoionized models, at least two possibilities have been proposed: a) shock waves (e.g., Peimbert, Sarmiento, & Fierro 1991, and references therein), and b) chemical abundance inhomogeneities (e.g., Torres-Peimbert, Peimbert, & Peña 1990, and references therein).

To study this problem further we have made use of the C line intensities compilation by Rola & Stasinska (1994). In § 2 we present the $T(C^{++})$ and $T(O^{++})$ temperatures and derive the $N(C^{++})/N(H^+)$ values based on these temperatures. In § 3 we study possible causes for the $T(O^{++})-T(C^{++})$ values. In § 4 we discuss why the abundances derived from $T(C^{++})$ should be preferred over those derived from $T(O^{++})$. The conclusions are presented in § 5.

2. TEMPERATURES AND C^{++}/H^+ ABUNDANCES

The $N(C^{++})/N(H^+)$ abundance ratio has been usually derived from the C^{++} $\lambda\lambda$1906, 1909 collisionally excited lines by means of

$$\frac{N(C^{++})}{N(H^+)} = 1.38 \times 10^{-7} T_4^{-0.25} \exp(7.543/T_4) \frac{I(1906+1909)}{I(H\beta)}, \tag{1}$$

where $T_4 = 10^{-4}T$, the C^{++} collisional excitation cross sections come from Pradhan & Peng (1995) and the Hβ recombination coefficient, $\alpha(H\beta)$, was obtained from Hummer & Storey (1987). The $I(1906)/I(1909)$ ratio changes from 1.5 to 0.05 when going from $N_e = 10^3$ to 10^6 cm^{-3} (e.g., Osterbrock 1989), alternatively $I(1906+1909)/I(H\beta)$ only varies by less than 3% for $N_e < 10^5$ cm^{-3} and by less than 10% for $N_e < 10^6$ cm^{-3}, therefore the density dependence for $N_e < 10^6$ cm^{-3} of equation (1) is negligible and has not been considered. The change in $I(1906)/I(1909)$ is due to collisional de-excitations of $\lambda(1906)$; most of these de-excitations end in the upper level of $\lambda(1909)$ leaving the $I(1906+1909)$ value almost unaffected.

It is also possible to derive the $N(C^{++})/N(H^+)$ ratio from the $C^+\lambda4267$ recombination line based on

$$\frac{N(C^{++})}{N(H^+)} = 0.109\, T_4^{0.14} \frac{I(4267)}{I(H\beta)}, \tag{2}$$

where $\alpha(4267)$ was obtained from Pengelly (see Seaton 1978). A more recent determination of $\alpha(4267)$ (Péquignot, Petitjean, & Boisson 1991) yields

$$\frac{N(C^{++})}{N(H^+)} = 0.0898\, T_4^{0.25} \frac{I(4267)}{I(H\beta)}. \tag{3}$$

The $N(C^{++})/N(H^+)$ value derived from equation (3) is 1.21 times smaller than that derived from equation (2) for $T_4 = 1$.

From the ratio of equations (1) and (3) it is possible to define a $T(C^{++})$ given by

$$\frac{I(1906+1909)}{I(4267)} = 6.51 \times 10^5\, T_4^{0.50}(C^{++}) \exp[-7.543/T_4(C^{++})]. \tag{4}$$

The sample in Table 1 includes the 67 entries from the compilation by Rola & Stasinska (1994) with measured $\lambda\lambda$1906 +1909, 4267, 4363, 4861 and 5007 line intensities; some of the entries correspond to the whole object while the multiple entries for a given object correspond to different positions in it. We have added NGC 2818 to the sample by adopting the λ4267 line intensity measured by Peimbert & Torres-Peimbert (1987). For NGC 6543 we have taken $I(1906+1909)/I(H\beta) = 0.12$ (Pwa, Mo, & Pottasch 1984) instead of the 3.53 value tabulated by Rola & Stasinska. From the line intensities of the sample and equation 4 we derived $T(C^{++})$; for $T(O^{++})$ we took the values of Rola & Stasinska with the exception of Hu 1–2 for which we took 19000 K (Peimbert and Torres-Peimbert 1987).

TABLE 1

TEMPERATURES AND (C^{++}/H^{+}) ABUNDANCES

Object	$T(C^{++})$	$T(O^{++})$	$N\left(\frac{C^{++}}{H^{+}}\right)^a$ (10^{-3})	$N\left(\frac{C^{++}}{H^{+}}\right)^b$ (10^{-3})	$N\left(\frac{C^{++}}{H^{+}}\right)^c$ (10^{-3})	f^d
NGC 40	8832.	10767.	0.400	0.420	0.082	4.88
NGC 1535–1	9464.	12301.	0.655	0.699	0.0891	6.68
NGC 1535–2	10549.	12149.	0.410	0.423	0.154	2.66
NGC 1535–3	10045.	12051.	0.360	0.376	0.098	3.67
NGC 2022	10419.	14227.	0.817	0.881	0.109	7.50
NGC 2371–2	9841.	13290.	0.617	0.664	0.078	7.91
NGC 2392–1	10408.	14483.	0.336	0.364	0.040	8.40
NGC 2392–2	10777.	14748.	0.110	0.118	0.015	7.33
NGC 2392–3	9444.	16127.	1.062	1.210	0.034	31.24
NGC 2392–4	11517.	15736.	0.167	0.181	0.027	6.19
NGC 2392–5	9041.	13767.	0.648	0.718	0.033	19.64
NGC 2440	12646.	14383.	0.381	0.392	0.180	2.12
NGC 2818	11658.	14928.	0.411	0.436	0.094	4.37
NGC 2867	10860.	11459.	0.825	0.835	0.567	1.46
NGC 3242–1	9498.	11738.	0.621	0.653	0.129	4.81
NGC 3242–2	10096.	11285.	0.522	0.536	0.231	2.26
NGC 3242-3	9818.	11383.	0.644	0.667	0.216	2.98
NGC 3242–4	10398.	11379.	0.472	0.482	0.247	1.91
NGC 3242–5	10596.	10846.	0.255	0.256	0.215	1.19
NGC 3918	11902.	14170.	0.403	0.420	0.140	2.88
NGC 6153	6985.	8689.	2.217	2.340	0.253	8.76
NGC 6210	7823.	9787.	0.422	0.447	0.058	7.28
NGC 6302	13985.	16998.	0.146	0.153	0.054	2.70
NGC 6543	7303.	8334.	0.548	0.568	0.148	3.70
NGC 6565	7879.	10467.	0.406	0.436	0.036	11.28
NGC 6572	9819.	9907.	0.358	0.358	0.333	1.08
NGC 6644	11155.	12769.	0.397	0.410	0.163	2.44
NGC 6720–1	10567.	11551.	0.464	0.474	0.247	1.88
NGC 6720–2	8994.	11339.	1.399	1.480	0.233	6.00
NGC 6720–3	10043.	11114.	0.899	0.921	0.425	2.12
NGC 6720–4	9809.	9982.	0.715	0.718	0.623	1.15
NGC 6720–5	9536.	9824.	0.586	0.590	0.461	1.27
NGC 6720–6	9928.	9334.	0.457	0.450	0.754	0.61
NGC 6720–7	9618.	9600.	0.685	0.685	0.695	0.99
NGC 6720–8	10243.	10298.	0.822	0.823	0.790	1.04
NGC 6741	11909.	11959.	0.535	0.534	0.521	1.03
NGC 6818	12646.	12989.	0.419	0.421	0.356	1.18
NGC 6826–1	9449.	9367.	0.221	0.221	0.238	0.93
NGC 6826–2	8516.	9405.	0.535	0.549	0.226	2.37
NGC 6826–3	8603.	9414.	0.432	0.442	0.199	2.17
NGC 6826–4	8530.	8853.	0.457	0.462	0.328	1.39
NGC 6826–5	8733.	8925.	0.443	0.446	0.366	1.21
NGC 6826–7	8054.	9152.	0.561	0.580	0.177	3.17
NGC 6853–2	9966.	11377.	0.987	1.020	0.373	2.65
NGC 6853–3	10941.	10901.	0.377	0.376	0.387	0.97
NGC 6853–4	9956.	9995.	0.816	0.817	0.792	1.03
NGC 6853–7	9258.	9019.	0.705	0.701	0.880	0.80

TABLE 1 (CONTINUED)

Object	$T(C^{++})$	$T(O^{++})$	$N\left(\frac{C^{++}}{H^+}\right)^a$ (10^{-3})	$N\left(\frac{C^{++}}{H^+}\right)^b$ (10^{-3})	$N\left(\frac{C^{++}}{H^+}\right)^c$ (10^{-3})	f^d
NGC 6886	13028.	13049.	0.422	0.421	0.418	1.01
NGC 7009–1	8218.	10505.	0.855	0.909	0.109	7.84
NGC 7009–2	8412.	9552.	0.516	0.533	0.172	3.00
NGC 7009–3	8121.	9962.	0.776	0.816	0.133	5.84
NGC 7009–4	8515.	9316.	0.466	0.477	0.213	2.19
NGC 7027	12431.	15022.	0.512	0.535	0.172	2.98
NGC 7662–1	11835.	14063.	0.328	0.341	0.114	2.88
NGC 7662–2	12244.	13400.	0.321	0.328	0.185	1.74
NGC 7662–3	12212.	12658.	0.330	0.333	0.264	1.25
NGC 7662–4	12267.	11919.	0.331	0.328	0.399	0.83
NGC 7662–5	12445.	11579.	0.304	0.298	0.487	0.62
IC 1297	9382.	10175.	0.557	0.568	0.292	1.91
IC 2003	11155.	11682.	0.406	0.410	0.296	1.37
IC 2149	8318.	10370.	0.652	0.688	0.103	6.33
IC 2165	12992.	15370.	0.575	0.598	0.225	2.56
IC 3568	10324.	11624.	0.226	0.233	0.097	2.33
Hu 1–2	12493.	19000.	0.285	0.316	0.032	8.91
J 320	13467.	12540.	0.193	0.190	0.298	0.65
J 900	12744.	12244.	0.792	0.783	1.020	0.78
Me2–1	12157.	13526.	0.453	0.464	0.235	1.93
SwSt 1	9865.	11109.	0.179	0.184	0.074	2.42

[a] Obtained with $T(C^+)$.
[b] Obtained with $T(O^{++})$, λ4267.
[c] Obtained with $T(O^{++})$, λ1909.
[d] The ratio of the fourth and the sixth columns.

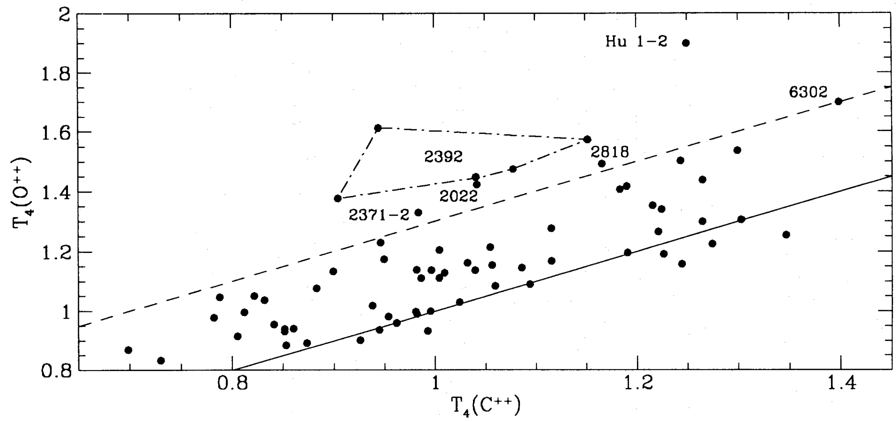

Fig. 1. $T(O^{++})$ vs. $T(C^{++})$ diagram. The solid line corresponds to $T(O^{++}) = T(C^{++})$, while the broken line to $T(O^{++}) - T(C^{++}) = 3000$ K. The five values for NGC 2392 are represented and joined by dash-dot lines.

From Table 1 and Figure 1 it can be seen that in general $T(C^{++}) < T(O^{++})$; an unexpected result under the assumption that these objects can be fitted by photoionization models. From detailed photoionization models it is expected that $T(O^{++}) \approx T(C^{++})$; for example, in the models for NGC 7662 of Harrington et al. (1982) $T(C^{++})$ is from 60 – 210 K higher than $T(O^{++})$.

Another way to look at the $T(O^{++})-T(C^{++})$ discrepancy is to study the $N(C^{++})/N(H^+)$ values. In Table 1 we also present the $N(C^{++})/N(H^+)$ values derived in three different ways: a) from $T(C^{++})$ and equation (1) or (3) that yield the same result, b) from $T(O^{++})$ and λ4267, and c) from $T(O^{++})$ and $\lambda\lambda$1906 + 1909. In Figure 2 we present the difference between the $N(C^{++})/N(H^+)$ values derived from $T(C^{++})$ versus the values derived from $T(O^{++})$ and $\lambda\lambda$1906 + 1909. Notice that the ratio of the two determinations, that we will define as f, varies from object to object and that the full range of the variation for the sample goes from $f = 31$ to $f = 0.6$. In what follows we will discuss possible causes for the $T(O^{++}) - T(C^{++})$ discrepancy.

3. POSSIBLE CAUSES FOR THE C ABUNDANCE DISCREPANCIES

There are at least six possible causes for the significantly higher $T(O^{++})$ than $T(C^{++})$ values: a) errors in the atomic parameters, b) observational errors, c) a contribution to $I(4363)$ due to recombinations and charge transfer reactions, d) density fluctuations, e) small amplitude temperature fluctuations, and f) large amplitude temperature fluctuations. We will analyze these six possibilities.

3.1. Errors in the Atomic Parameters

Kaler (1986) suggested that a change of a factor of 4 in the recombination coefficient of λ4267 or in the collisional excitation parameter of $\lambda\lambda$(1906 + 1909) could bring the $T(C^{++})$ values in agreement with $T(O^{++})$, or the C^{++} abundances derived with λ4267 and $T(O^{++})$ in agreement with those derived with $\lambda\lambda$1906+1909 and $T(O^{++})$.

We have derived the f values for the 36 PN in Table 1 from the ratio of the fourth to the sixth column and their average amounts to 3.79, where only the mean f value for those objects with multiple observations was considered. This value implies a somewhat smaller discrepancy than that found by Kaler (1986). There are four differences between the sample by Kaler and that in Table 1: a) the samples overlap but are not the same, Kaler had 30 objects while in Table 1 we consider 36, b) the effective recombination coefficient used in Table 1 is 21% higher than that used by Kaler, c) the λ4267 line intensities used in Table 1 tend to be smaller than those used by Kaler, probably due to observational errors, and d) the $\lambda\lambda$1906 + 1909 line intensities used in Table 1 tend to be higher than those used by Kaler, probably due to the different calibration procedure.

There are two arguments against the suggestion by Kaler as the only reason for the discrepancy: a) The difference between two independent computations of the recombination coefficient of λ4267 amounts to only

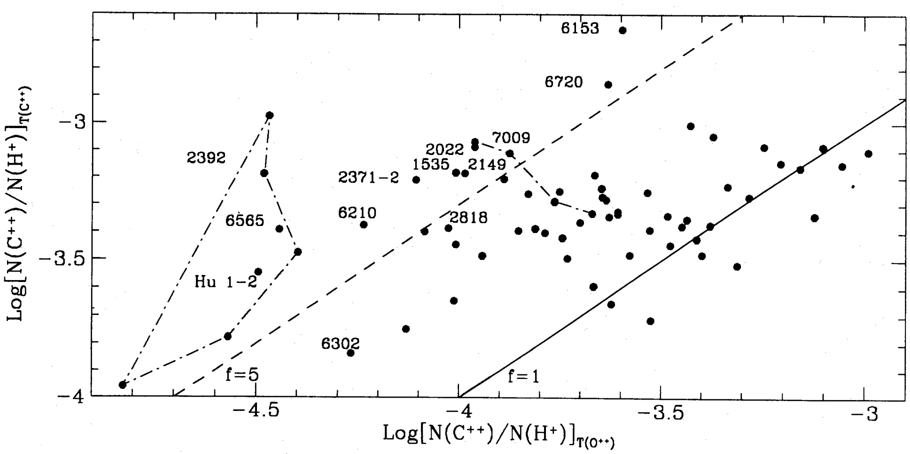

Fig. 2. Log $N(C^{++})/N(H^+)_{T(C^{++})}$ vs. log $N(C^{++},1908)/N(H^+)_{T(O^{++})}$ diagram. The solid line corresponds to $f = 1$, while the broken line to $f = 5$. The five values for NGC 2392 and the four values for NGC 7009 are joined together.

21% (Seaton 1978; Pequignot et al. 1991); a similar situation prevails with the collisional cross sections of $\lambda\lambda 1906 + 1909$ (Dufton et al. 1978; Mendoza 1983; Berrington 1985; Pradhan & Peng 1995). b) Even if an error of a factor of 4 were present in the atomic parameters it would be possible to fit the average f value but not the factor of 50 spread.

3.2 Observational Errors

In photographic observations the intensities of weak lines, like $\lambda 4267$ and $\lambda 4363$, have been overestimated relative to strong lines, like $\lambda 4861$ and $\lambda 5007$, this overestimation produces spuriously lower $T(\mathrm{C}^{++})$ and higher $T(\mathrm{O}^{++})$ values (e.g., Torres-Peimbert et al. 1980). This problem is well known and has been taken into account in later papers. It should be noted that the sample presented by Rola & Stasinska (1994) does not include photographic data.

Rola & Pelat (1994) have also shown that for emission lines with low signal-to-noise the intensity of weak lines tends to be systematically overestimated, the effect becomes important for S/N ~ 10 and increases for smaller S/N values. Most of the PN in Table 1 are very bright and the $\lambda\lambda 4363$, Hβ and 5007 observations have S/N values considerably higher than ten, therefore for these lines the effect can be neglected. Alternatively, $\lambda 4267$ is relatively faint and in some cases could have been observed with low S/N, this effect would go in the direction of reducing the $T(\mathrm{O}^{++}) - T(\mathrm{C}^{++})$ discrepancy; this effect could also affect the $\lambda\lambda 1906 + 1909$ intensities, but for these lines it would go in the opposite direction of what is needed to explain the $T(\mathrm{O}^{++}) - T(\mathrm{C}^{++})$ discrepancy. To evaluate the relevance of this effect we need to know the S/N values for each of the $\lambda 4267$ measurements, which is beyond the scope of this investigation; for future observations S/N values for weak lines should be presented.

3.3. Contribution to I(4363) Due to Recombination and Charge Transfer Processes

The O^{++} electron temperature can be derived from

$$T(\mathrm{O}^{++}) = \frac{32900}{\ln[0.1742 I(5007)/I(4363)]} \ , \tag{5}$$

where it has been assumed that $\lambda\lambda 4363$ and 5007 are excited by collisions only and the atomic parameters were taken from the compilation by Mendoza (1983). Some contribution to the intensity of $\lambda\lambda 4363$ and 5007 could be due to: a) charge transfer ($\mathrm{O}^{+3} + \mathrm{H}^0 \rightarrow \mathrm{O}^{+2} + \mathrm{H}^+$), b) radiative recombination, and c) dielectronic recombination. Such contribution would reduce the $T(\mathrm{O}^{++})$ values derived from equation (5).

Dalgarno & Sternberg (1982) have proposed that the contribution to $I(4363)^{Obs}$ due to charge transfer, $I(4363)^{CT}$, can be estimated from

$$I(4363)^{CT} = [0.63 + 1.99 k(^1P_0)/k(^1P)] I(5592) \ , \tag{6}$$

where $\lambda 5592$ is a permitted line of O^{+2}, $k(^1P)$ and $k(^1P_0)$ are the charge transfer rate coefficients into the ^1P and $^1P_0$ states; these coefficients have been computed by Dalgarno, Heil, & Butler (1981) for different temperatures. Moreover Shields, Dalgarno, & Sternberg (1983) mention that there appears to be no accessible autoionizing singlet level of O^{+2} so that dielectronic recombination is unlikely to be significant in the production of $I(5592)$. Consequently to derive $T(\mathrm{O}^{++})$ we should use

$$I(4363)^{Coll} = I(4363)^{Obs} - I(4363)^{CT} \ . \tag{7}$$

Dalgarno & Sternberg estimate that for NGC 2440 this effect amounts to 100 K. We have computed this effect for the PNe with measured $\lambda 5992$ by Aller & Walker (1970) and find that for all cases it amounts to less than 150 K.

Dalgarno & Sternberg (1982) find an upper limit of 200 K for the reduction of $T(\mathrm{O}^{++})$ in PNe due to dielectronic recombination of O^{3+} into the $2s2p^2nd\,^5P$ resonance states of O^{++}, followed by radiative transitions to the ^5S level.

In what follows these effects will not be considered.

3.4. Density Fluctuations

In the presence of density fluctuations it is possible to overestimate $T(\mathrm{O}^{++})$ if one adopts a low value for the density (Viegas & Clegg 1994). Clumps with $N_e \sim 10^6$ cm^{-3} superimposed to a general medium $N_e \sim 10^4$ cm^{-3}

are needed for this effect to be significant. We consider this possibility unlikely for most objects for the following reasons: a) A density contrast of two orders of magnitude implies that the recombination rate in the clumps will be four orders of magnitude higher than in the general medium; and consequently that the clumps might have a lower degree of ionization; probably most of the O would be in the form of O^+ or O^0. b) By comparing the densities derived from $I(3726)/I(3729)$, $N_e(3727)$, with those derived from $I(3726+3729)/I(7320+7330)$, $N_e(3727, 7325)$, it is possible to find out if density fluctuations are present; some objects with good line intensity measurements (e.g., Peimbert 1971) show evidence for $N_e(3727, 7325) > N_e(3727)$, implying the presence of density fluctuations, but the density fluctuations are not large enough to affect the $T(O^{++})$ determinations.

3.5. Small Amplitude Temperature Fluctuations

The topic of temperature fluctuations and their effect on the determination of temperatures and abundances was introduced by Peimbert (1967; see also Peimbert & Costero 1969).

The effect that temperature fluctuations have on a temperature derived from the ratio of two collisionally excited lines has been studied before (Peimbert 1967), alternatively the effect on a temperature derived from the ratio of a permitted line to a collisionally excited line has not, we will consider it below.

In general the intensity of a recombination line is proportional to a power of the temperature

$$I(r) \propto T^{\alpha} \quad , \tag{8}$$

while for a collisionally excited line it is proportional to

$$I(c) \propto T^{\beta} \exp(-\Delta E/kT) \quad , \tag{9}$$

where ΔE is the energy difference between the upper level of the collisionally excited transition and the ground level of the ion involved. In the presence of small temperature fluctuations the temperature can be expanded in a Taylor series about the mean temperature and the intensity of a recombination line is affected by

$$I(r) \propto T_0^{\alpha} \left[1 + \alpha(\alpha - 1)t^2/2\right] \quad , \tag{10}$$

where T_0 is the mean temperature of the emitting region and t is the rms temperature variation; T_0 and t^2 are given by (Peimbert 1967)

$$T_0 = \frac{\int T N_e N_i d\Omega d\ell}{\int N_e N_i d\Omega d\ell} \quad , \tag{11}$$

and

$$t^2 = \frac{\int (T - T_0)^2 N_e N_i d\Omega d\ell}{T_0^2 \int N_e N_i d\Omega d\ell} \quad , \tag{12}$$

where N_i is the ionic density, Ω is the observed solid angle and ℓ is the optical pathlength inside the nebula.

Similarly the intensity of a collisionally excited line is affected by

$$I(c) \propto \left[T_0^{\beta} \exp(-\Delta E/kT_0)\right] \left\{1 + \left[(\beta - 1)\left(\beta + \frac{2\Delta E}{kT_0}\right) + \left(\frac{\Delta E}{kT_0}\right)^2\right] \frac{t^2}{2}\right\} \quad , \tag{13}$$

therefore from equations (10) and (13) the intensity ratio of a collisionally excited line to a recombination line is given by

$$\begin{aligned} \frac{I(c)}{I(r)} &\propto \left[T_0^{\beta-\alpha} \exp(-\Delta E/kT_0)\right] \frac{\left\{1 + \left[(\beta-1)(\beta + 2\Delta E/kT_0) + (\Delta E/kT_0)^2\right](t^2/2)\right\}}{\left[1 + \alpha(\alpha - 1)(t^2/2)\right]} \\ &\propto T_0^{\beta-\alpha} \exp(-\Delta E/kT_0) \times \\ &\quad \left\{1 + \left[-\alpha(1-\alpha) + (\beta - 1)(\beta + 2\Delta E/kT_0) + (\Delta E/kT_0)^2\right](t^2/2)\right\} . \end{aligned} \tag{14}$$

On the other hand the temperature derived from the ratio of a collisionally excited line to a recombination line, $T(c/r)$, can be obtained from the following relationship

$$\frac{I(c)}{I(r)} \propto T(c/r)^{\beta-\alpha} \exp\left[-\Delta E/kT(c/r)\right]$$
$$\propto \left[T_0^{\beta-\alpha} \exp(-\Delta E/kT_0)\right] \left[1 + \left(\frac{T(c/r) - T_0}{T_0}\right)(\beta - \alpha + \Delta E/kT_0)\right]. \tag{15}$$

Consequently from equations (14) and (15) we have

$$T(c/r) = T_0 \left\{1 + \frac{\left[-\alpha(1-\alpha) + (\beta - 1)(\beta + 2\Delta E/kT_0) + (\Delta E/kT_0)^2\right](t^2/2)}{\left[\beta - \alpha + (\Delta E/kT_0)\right]}\right\}. \tag{16}$$

Equation (16) can be used to derive $T(1908/4267)$; for $I(1906{+}1909)$: $\beta = -0.62$ and $\Delta E/k = 7.543 \times 10^4$ K, while for $I(4267)4$: $\alpha = -1.12$. Therefore

$$T(\mathrm{C}^{++}) = T_0 \left\{1 + \frac{\left[(75430/T_0)^2 - 3.24(75430/T_0) - 1.37\right](t^2/2)}{(75430/T_0) + 0.50}\right\}. \tag{17}$$

Alternatively, for $T(4363/5007)$ we have (Peimbert 1967)

$$T(\mathrm{O}^{++}) = T_0 \left\{1 + \left[(90800/T_0) - 3\right](t^2/2)\right\}. \tag{18}$$

For typical values of T_0 in PNe equation (18) yields higher temperatures than equation (17), a result that could explain part of the differences observed. For example for $T_0 = 10\,000$ K equations (17) and (18) yield:

$$T(\mathrm{C}^{++}) = T_0(1 + 1.93\,t^2) \quad ,$$

$$T(\mathrm{O}^{++}) = T_0(1 + 3.04\,t^2) \quad ;$$

for $T(\mathrm{O}^{++}) - T(\mathrm{C}^{++}) \sim 2000$ K, it follows that $t^2 \sim 0.18$ which is an extremely large value, while equations (17) and (18) are based on the assumption of small amplitude temperature variations, i.e., $t^2 \ll 1$ or $t^2 < 0.1$.

To have a better representation of the temperature structure for objects with large $T(\mathrm{O}^{++}) - T(\mathrm{C}^{++})$ values, we need to know the mechanism that produces the temperature variations and the shapes of the temperature variations.

3.6. Large Amplitude Temperature Variations

The large $T(\mathrm{O}^{++}) - T(\mathrm{C}^{++})$ values could be due to the presence of photoionized and shocked regions inside PNe. Peimbert et al. (1991) combined spectra of shocked models with spectra of photoionized models to try to reproduce the emitting conditions of giant H II regions; they found that in the combined spectra the nebular to recombination line intensity ratios (3727/Hβ, 5007/Hβ, 6584/Hβ) were very similar to those of the photoionized models, while the auroral to nebular ratios (4363/5007) were greatly enhanced.

By combining shock models with photoionized models we will study the $I(4363)/I(5007)$ ratio and the effect on $T(\mathrm{O}^{++})$. Hartigan, Raymond, & Hartmann (1987) have produced a set of shock models with different physical characteristics. They present a set of line intensities for 13 different models. For all the models with shock velocities in the 100 to 400 km s^{-1} range (see models 1–6 and 9–13 in their Table 3) the $I(4363)/I(5007)$ ratios are higher by about an order of magnitude relative to photoionized models; moreover when combined with equation (5) yield temperatures in the 48 700 to 53 000 K range. The models with shock velocities of 50 km s^{-1} or less do not produce O^{++}. In this set of models $T(\mathrm{O}^{++})$ is almost independent of the shock velocity; $T(\mathrm{O}^{++})$ does not increase with shock velocity because at approximately the same temperature the O atoms become three times ionized. Therefore any combination of photoionization with shock wave models produces large temperature fluctuations and yields $T(O^{++})$ values higher than those predicted by photoionized models (e.g., Shields et al. 1981; Harrington et al. 1982). To produce an excess temperature of 1500 K from a combined model relative to a photoionized model, a contribution of 10 to 20% from the Hβ emission due to the shock model and the rest due to the photoionized model is required.

A higher $I(1906+1909)/I(4267)$ ratio yields a higher $T(C^{++})$ value [see equation (4)], therefore to have large $T(C^{++})$ values shock models are required to produce stronger $I(1906+1909)/I(H\beta)$ and weaker $I(4267)/I(H\beta)$ ratios than photoionized models. There are no shock models in the literature with λ4267 included, therefore we cannot compare $T(C^{++})$ with $T(O^{++})$. Nevertheless we expect that in shock models $T(C^{++}) < T(O^{++})$. The arguments are the following: a) Given the ionization potentials of C^+ (24.4 eV), C^{++} (47.9 eV), O^+ (35.1 eV) and O^{++} (54.9 eV), it follows that C^{++} is produced and destroyed by shocks at lower temperatures than O^{++}, consequently we expect the collisionally excited lines of C^{++} to originate in cooler regions than the O^{++} lines. b) From all the models by Hartigan et al. (1987) with shock velocities in the 100 to 400 km s^{-1} range it is found that the $I(1906 + 1909)/I(H\beta)$ ratio is in the 1.12 to 3.48 range, with an average value of 2.55, while photoionized models of objects with intermediate degree of ionization can easily predict similar or higher $I(1906+1909)/I(H\beta)$ ratios than shock models (e.g., Shields et al. 1981; Harrington et al. 1982). c) In a combined spectrum with 80% photoionized and 20% shocked components, the intensity of $\lambda(4267)$ would be dominated by the photoionized component; moreover due to the ionization potentials of He^0 (24.6 eV), He^+ (54.4 eV), C^+ (24.4 eV) and C^{++} (47.9 eV), λ4267 is expected to behave like the He I lines and since the intensity of $I(5876)/I(H\beta)$, in the models of Hartigan et al. (1987), is very similar to that of photoionized models (e.g., Shields et al. 1981; Harrington et al. 1982), it follows that $I(4267)/I(H\beta)$ will be also similar; therefore we do not expect significant differences in the $I(4267)/I(H\beta)$ ratios between photoionized models and combined models.

4. DISCUSSION

In a recent study of the C abundances in PNe Rola & Stasinska (1994) suggested that the $T(O^{++})-T(C^{++})$ differences were mainly due to observational errors and that an additional part of the differences was due to spatial temperature variations. In this paper we argue that, for most objects, most of the $T(O^{++}) - T(C^{++})$ difference is real; but it is also possible that part of the difference for most objects and all of the difference for some of them could be due to observational errors. In what follows we will present arguments in favor of real $T(O^{++}) - T(C^{++})$ differences.

We present in Figure 1, based on Table 1, a plot of $T(O^{++})$ vs. $T(C^{++})$. From this figure it follows that most objects show $T(O^{++}) > T(C^{++})$ and that the average difference is 1480 K, considerably higher than the typical error in $T(O^{++})$ that amounts to about 300 K. Moreover, there are six objects with $T(O^{++})-T(C^{++}) > 3000$ K, including the five positions of NGC 2392 that are joined together. Four of the six objects are PNe of Type I: NGC 2371–2, NGC 2818, NGC 6302 and Hu 1–2, and show complex gas motions (e.g., Sabbadin, Bianchini, & Hamzaoglu 1982; Sabbadin 1984) indicating the presence of shock waves. The gas motions in NGC 6302 reach velocities of a few hundred km s^{-1} (Meaburn & Walsh 1980), and the line intensity ratios of [S II] and [N II] relative to Hα for this object indicate that there are regions across the face of the nebula dominated by shocks and others by photoionization (Bohigas 1994); moreover Rowlands, Houck, & Herter (1994) find that the highly ionized regions of NGC 6302 show higher T_e values than those predicted by photoionization models and conclude that the difference is due to mechanical energy input produced by shocks. NGC 2392, the Eskimo Nebula, also shows a complex velocity field that reaches velocities as high as 190 km s^{-1} relative to the central star; this velocity field is also indicative of shocks (O'Dell, Weiner, & Chu 1990).

In Figure 2 we present a plot of columns 4 and 6 of Table 1. Notice that for most objects $f > 1$. We also present a solid straight line with $f = 1$ and a broken straight line with $f = 5$. In addition to NGC 6302 and NGC 2818 we have also labeled all those objects with $f > 5$, we will describe them briefly. NGC 2371-2, NGC 2392 and Hu 1–2 were mentioned before. NGC 6153 and NGC 6565 are also Type I PN (Pottasch, Dennefeld, & Mo 1986; Aller, Keyes, & Feibelman 1988). Balick et al. (1994) find fast low ionization emission regions, "Fliers", in NGC 7009; Fliers show the ionization structure expected of bow shocks. Liu et al. (1995) based on O^+ recombination lines derived for NGC 7009 a $N(O^{++})/N(H^+)$ value a factor of 4.7 higher than that derived from forbidden lines under the assumption that $t^2 = 0.00$; to reconcile both C^{++}/H^+ values, a $t^2 = 0.098$ is needed. IC 2149 has been classified as an early type butterfly, while NGC 6210 as a peculiar lumpy PN consisting of many knots (Balick 1989). NGC 1535 presents only one region out of three with $f > 5$ and NGC 6720 only one region out of eight with $f > 5$.

In Figure 3 we plot columns 5 and 6 of Table 1 vs. $T(O^{++})$; the difference between $N(C^{++}, 4267)/N(H^+)$ and $N(C^{++}, 1908)/(N(H^+)$ increases with increasing $T(O^{++})$ which is consistent with the idea that the higher $T(O^{++})$ the higher the contribution of mechanical energy to the λ4363 line intensity. Also in Figure 3 we plot

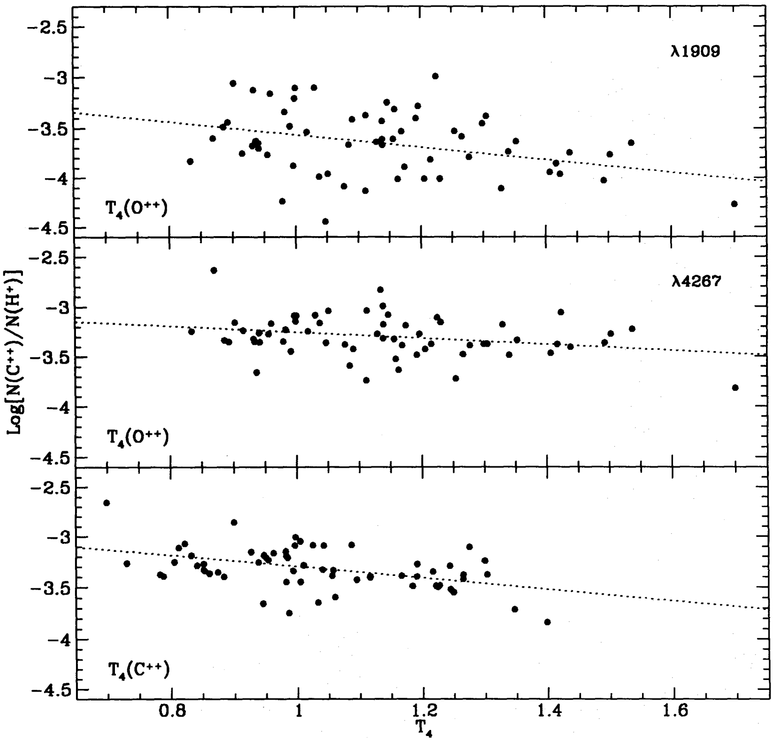

Fig. 3. $N(C^{++})/N(H^+)$ vs. temperature diagram. The sample is the same for the three panels. In the first panel the C^{++} abundance is derived from the $\lambda\lambda1906+1909$ lines and $T(O^{++})$, in the second panel from $\lambda4267$ and $T(O^{++})$ and in the third panel from $\lambda4267$ and $T(C^{++})$. We recommend the C^{++}/H^+ values of the third panel.

column 4, $N(C^{++})/N(H^+)$, vs. $T(C^{++})$, notice that the spread in the $N(C^{++})/N(H^+)$ values is considerably smaller than in the $N(C^{++}, 1908)/(N(H^+)$ values derived with $T(O^{++})$.

Liu & Danziger (1993) determined the Balmer continuum temperature, T(Bac), based on the ratio of the Balmer continuum to a Balmer emission line. For their sample of 16 PNe they find that $\langle T(O^{++}) - T(\mathrm{Bac})\rangle =$ 1475 K in excellent agreement with the $\langle T(O^{++}) - T(C^{++})\rangle = 1480$ K value for the sample presented in Table 1. In Table 2 we present the T(Bac) values for the three objects in common with Table 1 with the smallest observational errors; in particular note that for NGC 2392 the difference between $T(O^{++})$ and T(Bac) reaches 4σ. We also present in Table 2 the temperatures derived by Peimbert, Luridiana, & Torres-Peimbert (1995) from the ratio of different He I lines, where the differences between $T(O^{++})$ and T(He I) for NGC 7009 and Hu 1–2 reach 5σ and 12σ respectively. It is also possible to derive a temperature from the ratio of O II $\lambda4649$ to [O III] $\lambda5007$, $T(4649/5007)$, using a relation analogous to equation (4), based on the atomic data presented by Mendoza (1983) and Storey (1994). From the paper by Liu et al. (1995a) we have derived $T(4649/5007)$ for NGC 7009 and is presented in Table 2; notice that it is considerably smaller than $T(O^{++})$.

From Table 2 it follows that while $T(C^{++})$, T(Bac), T(He I) and $T(4649/5007)$ show similar values, $T(O^{++})$ is significantly higher than the other four. Furthermore preliminary results for other objects also show relatively strong $I(4649)/I(5007)$ values (Liu et al. 1995b; Kingsburgh & López 1995) that imply $T(4649/5007)$ values considerably smaller than $T(O^{++})$.

To summarize, there are several reasons that indicate that the $T(O^{++}) - T(C^{++})$ difference is real and probably due to temperature fluctuations. On the theoretical side: a) in the presence of small temperature fluctuations $T(C^{++})$ is closer to the average temperature, T_0, than $T(O^{++})$, b) shock waves affect considerably $I(4363)/I(5007)$, c) shock waves possibly affect more $I(4363)/I(5007)$ than $I(1906+1909)/I(4267)$, but detailed models are needed to test this statement. On the observational side: a) those objects with higher velocity

TABLE 2

OTHER TEMPERATURE DETERMINATIONS

Objects	$T(O^{++})$	$T(C^{++})$	T(Bac)	T(He I)	$T(4649/5007)$	Source
NGC 2392	15100	10237	8950^{+1350}_{-1070}	...	...	1,2,3
NGC 3242	11900	10081	9140^{+860}_{-720}	...	...	1,2,3
NGC 7009	10000	8317	8760^{+1460}_{-1120}	8000 ± 400	7300 ± 300	1,2,3,4,5
Hu 1-2	19000	12493	...	13000 ± 500	...	1,2,4

(1) This paper, (2) Rola & Stasinska 1994, (3) Liu & Danziger 1993, (4) Peimbert et al. 1995, (5) Liu et al. 1995a.

dispersions are the ones with higher $T(O^{++})-T(C^{++})$ values, suggesting the presence of shocks, b) $T(C^{++})$ is closer to the temperatures derived from the Balmer continuum than to $T(O^{++})$, c) for NGC 7009 and Hu 1–2 $T(C^{++})$ is closer to the temperatures derived from the He I lines than to $T(O^{++})$, d) for NGC 7009 $T(C^{++})$ is closer to $T(4649/5007)$ than to $T(O^{++})$.

Additional evidence in favor of shocks produced by the interaction of the stellar wind with previously ejected material from PNe has been presented elsewhere (Peimbert 1995, and references therein).

5. CONCLUSIONS

From the sample presented in Table 1 it is found that in general $T(O^{++}) > T(C^{++})$ and that $\langle T(O^{++}) - T(C^{++})\rangle = 1480$ K. Type I PNe and NGC 2392 show typical differences of about 3000 K; for Hu 1–2, a Type I PN, the difference reaches 6500 K.

Photoionized models predict that $T(O^{++}) \leq T(C^{++})$. In a medium where C^{++} and O^{++} coexist it is found that in the presence of spatial temperature fluctuations $T(O^{++}) > T(C^{++})$.

The objects with largest $T(O^{++})-T(C^{++})$ values are those that show complex gas motions, that often reach velocities higher than 100 km s^{-1}. The complex velocity fields support the idea that shocks are responsible for most of the $T(O^{++}) - T(C^{++})$ difference.

The average ratio between the C^{++}/H^+ abundances derived from λ4267/ Hβ with $T(C^{++})$ or $T(O^{++})$ relative to those derived from $I(1906 + 1909)/I(H\beta)$ together with $T(O^{++})$ amounts to $f = 3.8$. The objects with $f > 5$ are in general those that show the highest velocities and more complex velocity structures.

In the presence of a combination spectrum with photoionized and shock ionized components the $I(4363)/I(5007)$ and $I(4363)/I(H\beta)$ values are strongly affected while the $I(5007)/I(H\beta)$ value is not. Based on the agreement among $T(C^{++})$, T(Bac), T(He I), and $T(4649/5007)$, for well observed objects we recommend the use of $T(C^{++})$, T(He I), T(Bac) or $T(4649/5007)$ instead of $T(O^{++})$ to derive the $N(O^{++})/N(H^+)$ value from $I(5007)/I(H\beta)$.

The $N(C^{++})/N(H^+)$ values derived from $I(4267)/I(H\beta)$ are almost independent of the temperature structure because to a first approximation the recombination lines are proportional to T^{-1} and the temperature dependence of the ratio cancels out, therefore in the presence of large temperature fluctuations the $N(C^{++})/N(H^+)$ values derived from $I(4267)/I(H\beta)$ are more reliable than those derived from $I(1906 + 1909)/I(H\beta)$ and $T(O^{++})$. Similarly the $N(O^{++})/N(H^+)$ abundances derived from recombination lines should be more reliable than those derived from $I(5007)/I(H\beta)$ and $T(O^{++})$.

To advance further in this problem we need: a) a set of shock models including the C II λ4267 and O II λ4649 recombination lines, b) measurements of λ4267 and λ4649 with high S/N, and c) to determine $N(C^{++})/N(H^+)$ and $N(O^{++})/N(H^+)$ based on recombination lines.

It is a pleasure to acknowledge a critical reading of an earlier version of this paper by G. Stasinska as well as fruitful discussions with V. Escalante. We are grateful for grants DGAPA-UNAM 100693 and CONACyT F-113-E9201.

REFERENCES

Aller, L.H., & Walker, M.F. 1970, ApJ, 161, 917

Aller, L.H., Keyes, C.D., & Feibelman, W.A. 1988, PASP, 100, 192

Balick, B. 1989, in IAU Symp. 131, Planetary Nebulae, ed. S. Torres-Peimbert (Dordrecht: Kluwer), p. 83

Balick, B., Perinotto, M., Maccioni, A., Terzian, Y., & Hajian, A. 1994, ApJ, 424, 800

Berrington, K.A. 1985, J. Phys. B., 18, L395

Bohigas, J. 1994, A&A, 288, 617

Dalgarno, A., & Sternberg, A. 1982, ApJ, 257, L87

Dalgarno, A., Heil, T.G., & Butler, S.E. 1981, ApJ, 245, 793

Dufton, P.L., Berrington, K.A., Burke, P.G., & Kingston, A.E. 1978, A&A, 62, 111

Harrington, J.P., Seaton, M.J., Adams, S., & Lutz, J.H. 1982, MNRAS, 199, 517

Hartigan, P., Raymond, J., & Hartmann, L. 1987, ApJ, 316, 323

Hummer, D.G., & Storey, P.J. 1987, MNRAS, 224, 801

Kaler, J.B. 1986, ApJ, 308, 337

Kingsburgh, R.L., & López, J.A. 1995, in preparation

Liu, X.-W., & Danziger, I.J. 1993, MNRAS, 263, 256

Liu, X.-W., Storey, P.J., Barlow, M.J., & Clegg, R.E.S. 1995a, MNRAS, 272, 369

_______. 1995b, in preparation

Meaburn, J., & Walsh, J.R. 1980, MNRAS, 191, 5P

Mendoza, C. 1983, in IAU Symp. 103, Planetary Nebulae, ed. D.R. Flower (Dordrecht: Reidel), p. 143

O'Dell, C.R., Weiner, L.D., & Chu, Y.-H. 1990, ApJ, 362, 226

Osterbrock, D.E. 1989, Astrophysics of Gaseous Nebulae and Active Galactic Nuclei (University Science Books)

Peimbert, M. 1967, ApJ, 150, 825

_______. 1971, Bol. Obs. Tonantzintla y Tacubaya, 6, 21

_______. 1995, in The Analysis of Emission Lines, ed. R.E. Williams & M. Livio (Cambridge: Cambridge Univ. Press), in press

Peimbert, M., & Costero, R. 1969, Bol. Obs. Tonantzintla y Tacubaya, 5, 3

Peimbert, M., Luridiana, V., & Torres-Peimbert, S. 1995, RevMexAA, 31, 147

Peimbert, M., Sarmiento, A., & Fierro, J. 1991, PASP, 103, 815

Peimbert, M., & Torres-Peimbert, S. 1987, RevMexAA, 14, 540

Péquignot, D., Petitjean, P., & Boisson, C. 1991, A&A, 251, 680

Pottasch, S.R., Dennefeld, M., & Mo, J. 1986, A&A, 155, 397

Pradhan, A.K., & Peng, J. 1995, in The Analysis of Emission Lines, ed. R.E. Williams & M. Livio (Cambridge: Cambridge Univ. Press), in press

Pwa, T.H., Mo, J.E., & Pottasch, S.R. 1984, A&A, 139, L1

Rola, C., & Pelat, D. 1994, A&A, 287, 676

Rola, C., & Stasinska, G. 1994, A&A, 282, 199

Rowlands, N., Houck, J.R., & Herter, T. 1994, ApJ, 427, 867

Sabbadin, F. 1984, A&AS, 58, 273

Sabbadin, F., Bianchini, A., & Hamzaoglu, E. 1982, A&AS, 50, 523

Seaton, M.J. 1978, in IAU Symp. 76, Planetary Nebulae, ed. Y. Terzian (Dordrecht: Reidel), 131

Shields, G.A., Aller, L.H., Keyes, C.D., & Czyzak, S.J. 1981, ApJ, 248, 569

Shields, G.A., Dalgarno, A., & Sternberg, A. 1983, Physical Review A, 28, 2137

Storey, P.J. 1994, A&A, 282, 999

Torres-Peimbert, S., Peimbert, M., & Daltabuit, E. 1980, ApJ, 238, 133

Torres-Peimbert, S., Peimbert, M., & Peña, M. 1990, A&A, 233, 540

Viegas, S.M., & Clegg, R.E.S. 1994, MNRAS, 271, 993

Valentina Luridiana, Manuel Peimbert, and Silvia Torres-Peimbert: Instituto de Astronomía, UNAM, Apartado Postal 70-264, 04510 México, D.F., México. (peimbert@astroscu.unam.mx).